Water Research 221 (2022) 118766

Contents lists available at ScienceDirect

Water Research

journal homepage: www.elsevier.com/locate/watres

Identification of priority areas for water ecosystem services by a techno-economic, social and climate change modeling framework

Ziqian Zhu [a,b], Kang Wang [a,b], Manqin Lei [a,b], Xin Li [a,b], Xiaodong Li [a,b], Longbo Jiang [a,b], Xiang Gao [a,b], Shuai Li [a,b], Jie Liang [a,b,*]

[a] College of Environmental Science and Engineering, Hunan University, Changsha 410082, PR China
[b] Key Laboratory of Environmental Biology and Pollution Control (Hunan University), Ministry of Education, Changsha 410082, PR China

ARTICLE INFO

Keywords:
Priority areas
Water-related ecosystem services
SWAT
MaxEnt
Marxan
Climate change

ABSTRACT

Water scarcity and quality deterioration often occur in economically developing regions, particularly during crises related to climate change or increasing human activities. The assignment of priority areas is considered a suitable strategy for stakeholders to mitigate water crises and cope with water stress. However, most studies focused on protecting water bodies in priority areas and did not consider the hydrological/hydrochemical/hydroecological interaction between aquatic and terrestrial ecosystems. We divided a watershed into manageable areas to select priority areas for multiple water-related ecosystem services (WES-priority areas), considering the aquatic-terrestrial interactions to predict the effects of climate change and human activities. The proposed novelty framework couples the soil and water assessment tool and maximum entropy models with a systematic conservation planning tool. It uses the gross domestic product as the economic cost to assess dynamic changes and social-environmental driving forces. A case study is conducted in the Xiangjiang River basin, a modified watershed of the main tributary of the Yangtze River, China. Results revealed that most of the WES-priority areas were located in the southern and southeastern regions of the upper reaches in all climatic scenarios. The conservation efficiency of the WES-priority areas decreased from 1.264 to 0.867 in 50 years, indicating that the level of protection declined as climate change accelerated. The precipitation was positively correlated with the WES-priority area selection in all climate scenarios. The temperature was only negatively correlated with the WES-priority areas when it exceeded 20 °C, and this effect became more pronounced as the temperature increased. The topographic factors had the most crucial impacts on the upstream priority areas selection. The water flow regulation service played a leading role in identifying WES-priority areas in the middle reaches because the priority areas' distribution here was closely related to the water yield, and its proportion decreased with the acceleration of global warming. The number of WES-priority areas was relatively low in the lower reaches. It was positively associated with the gross domestic product and the amount of built-up land. The proposed framework for WES-priority areas identification enables a sound trade-off between environmental protection and economic development.

1. Introduction

Water scarcity and water quality deterioration represent global threats to human society (Mekonnen and Hoekstra, 2016). The rise of the world population, improvement in living standards, change in the consumption structure, and an increase in irrigated agriculture are the main drivers of the increasing worldwide water crisis. An effective strategy to deal with complex water health problems is to develop separate control strategies for different river reaches and categorize rivers with similar water quality or societal demands in the same water function zone (Huang et al., 2010).

The goal of assigning water function zones is to set water quality and quantity targets; however, the ecological protection of the water source is rarely considered, stemming from the misunderstanding of the water conditions required to support freshwater ecosystems (Richter et al., 2003). Therefore, ecological protection has received increasing attention in the design of water protection schemes. Aquatic ecological processes are affected in several ways. Most ecological responses (energy

* Corresponding author at: College of Environmental Science and Engineering, Hunan University, Changsha 410082, PR China.
E-mail address: liangjie@hnu.edu.cn (J. Liang).

https://doi.org/10.1016/j.watres.2022.118766
Received 30 March 2022; Received in revised form 14 June 2022; Accepted 15 June 2022
Available online 16 June 2022

flow, fish survival, recruitment, and community structure) are related to the flow (Rosenfeld, 2017). In addition to hydrological processes, the surface water quality affects the ecological environment in various reaches to different degrees due to the adaptability of the aquatic organism to the environment (Luo et al., 2020). Due to the complex interactions between hydrology and hydrochemistry in aquatic ecosystems, a new method for partitioning water function zones is needed.

Another major drawback of the current river zoning law is that the division of water function zones was designed for water pollution monitoring and management of the river channels, whereas land-based activities surrounding the water have been ignored. Nevertheless, some land-based activities may have a considerable influence on water. Recent studies have shown that changes in the terrestrial landscape have significant impacts on neighboring aquatic ecosystems. The conversion of natural landscapes often affects nutrient fluxes, soil integrity, and native species communities. This change will affect the hydrology of the basin by changing the rate of interception, evapotranspiration, infiltration, and groundwater recharge, resulting in changes in the timing and amount of river runoff (Baker and Miller, 2013). On the other hand, water-based activities may also have several important consequences for the terrestrial ecosystem. For example, agricultural water consumption accounts for 70% of China's total water consumption, representing an important part of the social water cycle (Jiang, 2009). The water demand by the industry is also the key factor influencing the local socio-economic development level (de Loë et al., 2016). Thus, the stakeholders must develop an approach that integrates aquatic and terrestrial ecosystems to address the dynamics of the complex processes.

Conservation prioritization could provide useful information for selecting priority areas to protect aquatic and terrestrial ecosystems by considering the economic values of water-related ecosystem services (WES) (Liang et al., 2021). Globally, water provides multiple economic values by providing drinking water and water for industrial and agricultural production (Wei et al., 2017). Some ecosystem services are closely linked to many hydrological processes positively (e.g., water quality for fish raising) or negatively (e.g., water erosion) (Maes et al., 2009). To provide information for water resource management, the water yield, the soil retention, and the water purification are the commonly used WES when considering the level of ecosystem services in certain regions, as those parameters represent the hydrological and hydrochemical factors involved in water demands.

Since WES are spatially heterogeneous, and many synergies exist, the trade-offs are complicated and should be considered carefully to obtain a cost-effective solution (Balkanlou et al., 2020). Many conservation tools have been developed to select sites with a high conservation value and perform systematic conservation planning. As one of the most commonly used conservation tools, the systematic conservation planning tool Marxan has been widely applied to identify priority areas related to ecosystem services or wild habitats and exhibits excellent performance in identifying priority areas based on the principle of complementarity (He et al., 2021). However, studies on the selection of priority areas with specific ecosystem services have mostly focused on assessing ecosystems services values by obtaining rough statistical data from public institutions rather than combining specific relevant models. Besides, most Marxan modeling studies on habitat conservation frequently used climatic parameters as the primary factors affecting species distribution, whereas the hydrological and hydrochemical factors were rarely considered. However, studies have demonstrated that the hydrological regime substantially influences the distribution of freshwater fish (Hockley et al., 2014). Moreover, the priority area identification procedures that consider both economic and ecological values of WES have rarely been applied to different regions.

To obtain more accurate and concise data representing WES in the whole river basin, some hydrological models could be utilized (Malekian et al., 2019). The soil and water assessment tool (SWAT) is a semi-distributed and continuous ecohydrological model. It has been utilized to simulate hydrological and hydrochemical output variables that could be regarded as indicators to evaluate WES (Schmalz et al., 2016). Since the hydroecological related WES are important for arranging function zones, the species distribution model could be used to simulate the geographic distribution of aquatic species. The maximum entropy model (MaxEnt) is commonly used because of its outstanding performance with limited data (Kim et al., 2020). It has been broadly utilized for modeling fish distribution in freshwater to assess river health, conserve species, and identify priority areas (Frederico et al., 2014). Thus, the MaxEnt model was used in our study to estimate fish distribution as one WES. Studies have shown that excessive nitrogen and phosphorus inputs may lead to water eutrophication, causing oxygen level reduction because of the accumulation and decomposition of organic matter and leading to the suffocation of many fish and macroinvertebrates (Hockley et al., 2014). Besides, sediment deposits may impact some developmental stages of fish, killing roe and destroying the gills of older fish (Sutherland and Meyer, 2007). Thus, we input the output variables from SWAT as some of the environmental factors into MaxEnt because those WES could affect fish distribution.

This study was conducted in a modified watershed in the Xiangjiang River basin (XRB). The XRB is a major sub-watershed of the Yangtze River and the primary rice-growing area in southern China (Tian et al., 2018). Due to multiple factors, such as climate change, rapid urbanization, and human-induced activities, the local water ecosystem services in the XRB have been severely degraded in recent years (Liang et al., 2020). Conflicts between humans and nature are common in this area; for example, it is difficult to balance the sustainability of the natural river ecosystem and economic development (Liang et al., 2018). Thus, the XRB is an ideal and representative area to investigate the selection of priority areas for WES. The results are significant for maintaining water ecological security and sustainable economic and social development in China (Xu et al., 2017).

In this study, a novelty framework is proposed to integrate WES into the selection of priority areas using water-land function zoning under climate change. Furthermore, the processes of hydrology/hydrochemistry/hydroecology in the integrated terrestrial−aquatic system are also considered to ensure healthy aquatic and terrestrial ecosystems. The objectives of this study are to (1) quantify WES in different climate scenarios, (2) determine the WES-priority areas cost-effectively, and (3) investigate the impacts of social-environmental factors on the WES-priority area's selection. Within this framework, the WES are quantified to support planning and decision-making regarding water resources protection in response to climate change.

2. Study area

The study was carried out in the XRB (Fig. 1). The Xiangjiang River is the main tributary of the middle and lower reaches of the Yangtze River. The XRB covers an area of 94,660 km^2 with a mainstream river length of 842 km. The mean elevation of the XRB is 326 m, with an average slope of 0.0134%. The XRB is located in the subtropical humid monsoon climate zone and experiences a hot, humid, and wet climate with an annual mean temperature of 16–18 °C and annual precipitation ranging from 1300 mm to 1600 mm. The area is heavily influenced by the monsoon, with most of the rainfall occurring in the summer from April to September. The Xiangjiang River originates from Jingfengling Mountain, and descends northward into the Yangtze River; it passes through diverse landscapes. The upper watershed is covered by alpine forests (63%), the middle reaches pass through an agriculture belt (30%), and the lower reaches meander through densely populated urban cities (2.7%). More than half of the habitants of the Hunan Province live in the XRB, thus the river is the undisputed mother river of 30 million residents, providing WES to both local economic and domestic water demands.

Because the selected watershed is relatively big, spatial heterogeneity can be taken into consideration when selecting proper priority

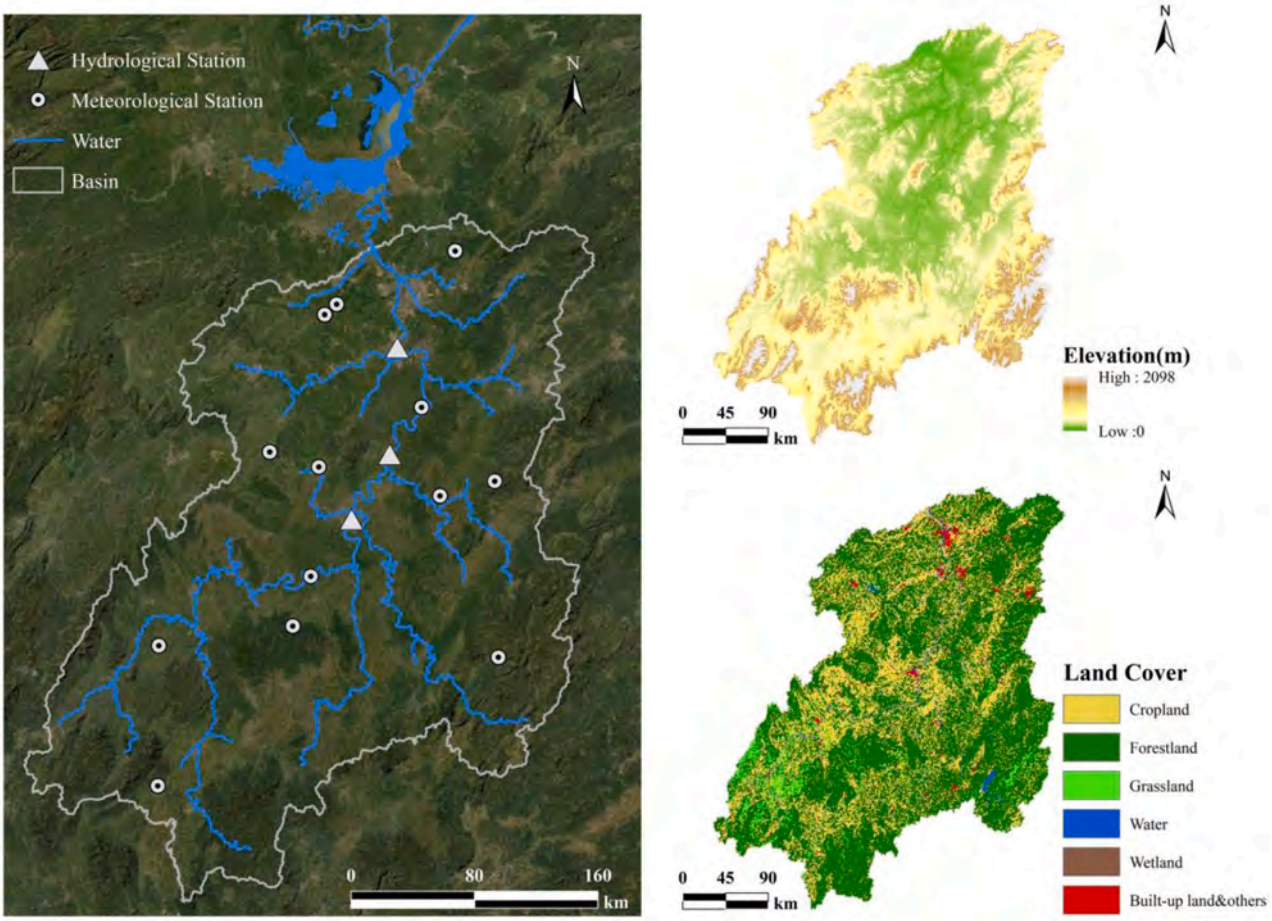

Fig. 1. The map of the Xiangjiang River basin in the southcentral part of China showing the location of the gage stations and the land cover (2010).

areas. A larger spatial scale will increase the comprehensive evaluation of research results considering the complexity and environmental heterogeneity of aquatic-terrestrial systems. The diverse landscape patterns throughout this river basin provide an excellent system for investigating WES-priority area determination, simultaneously considering the complex impacts of hydrological, hydrochemical, and ecological factors under various landscapes. Moreover, the studied area contains some regions that are undergoing the largest wave of rapid urbanization in

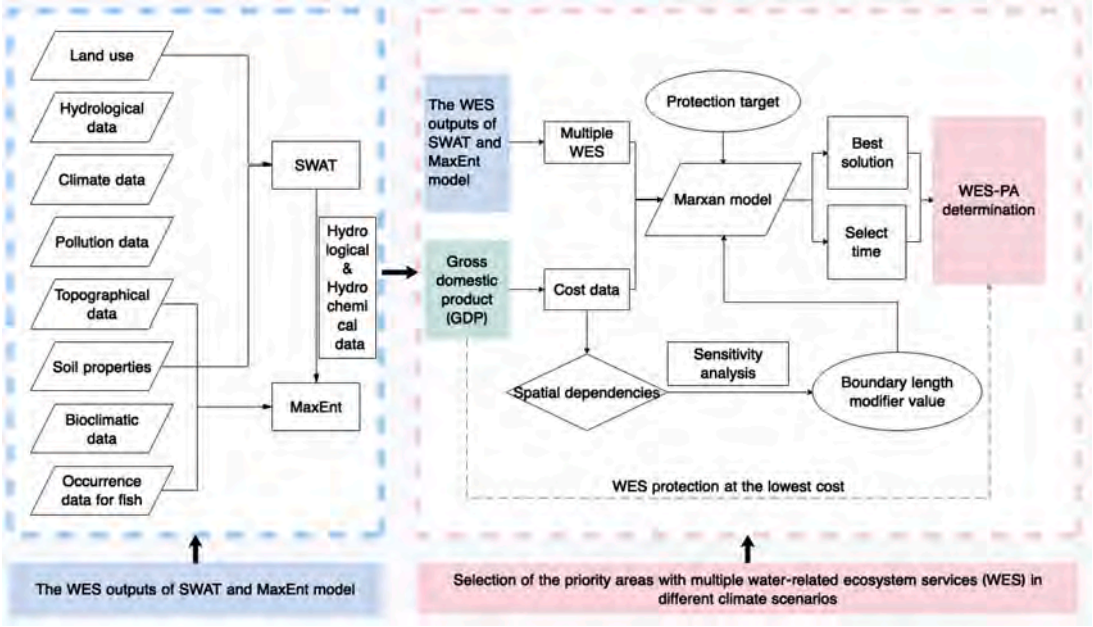

Fig. 2. The coupled methodological framework for identifying multiple water-related ecosystem services in the priority areas (WES-priority areas).

human history, which is one of the typical systems to reflect the impact of human activities on the WES, providing insight into the priority areas' distribution with complex anthropogenic influence. The study for WES-priority areas identification in XRB reflects a sound trade-off between environmental protection and economic development. In summary, we think our findings have implications with regard to both the XRB case and other cases that have been facing a global warming crisis.

3. Materials and methodology

The proposed framework (Fig. 2) consists of the following steps: data preprocessing, future climate projections, the establishment, calibration, and validation of SWAT (Fig. S1), the establishment of the MaxEnt model to assess the fish distribution, and the systematic conservation planning for WES using the Marxan model, and the redundancy analysis to investigate the influence of climate change and social-environmental factors on the WES-priority areas. The identification of WES-priority areas while considering climate change provides an effective trade-off framework for environmental protection and economic development.

3.1. Data sources

The data inputs and sources are summarized in Table 1. The land use data were reclassified to fit the categories of the SWAT. The soil data were used to determine the soil properties, and a digital elevation model was used to delineate the XRB watershed in the SWAT simulation. The nitrogen and phosphorus pollution inputs containing crop cultivation, scattered small-scale animal feedlot operations, and rural sewage were calculated based on the Hunan Statistic Yearbook. During the establishment of SWAT, we used a threshold of 100,000 ha and delineated 53 sub-basins, which were further divided into 621 HRUs.

The daily weather records at 13 stations in the XRB from 1997 to 2015 were obtained from the China Meteorological Administration to simulate the daily weather in the SWAT. The daily discharge at the hydrological stations (Hengyang, Hengshan, and Xiangtan), monthly sediment transport at the Xiangtan station from 1997 to 2015, and the monthly water quality at this station from 2005 to 2015 were obtained from the hydrological department of Hunan province (Fig. 1) to calibrate and validate the results of SWAT.

The future climate projections (average for 2041–2060, hereafter referred to as 2050; average for 2061–2080, hereafter referred to as 2070) were downloaded from the WorldClim website to process the future climatic scenarios in SWAT and MaxEnt models. The climate change scenarios in 2050 and 2070 were identical to the Representative Concentration Pathway (RCP) 4.5 emission scenario at 30 s resolution (1 km) of the General Circulation Model (GCM) (Mirdashtvan et al., 2018). The transient climate projections for 1997–2080 were separated into several time slices in SWAT and MaxEnt operation: 1997–2015 was considered the baseline scenario, 2050 was the mid-term scenario, and 2070 was the long-term scenario.

The geographic coordinates of the feature locations were used in the MaxEnt model. The data were acquired from the Hunan Aquatic Ecological Monitoring Programs. To evaluate the potential effects of climate change on fish distribution in the XRB, we used 19 bioclimatic variables from the HadGEM2-AO model in the WorldClim database. The topographic data and the soil categories with chemical and physical properties were the same in the MaxEnt model and the SWAT model. The computational results of the SWAT, including the WYLD, SYLD, ORGN, and ORGP in the XRB, were used as input hydrological and hydrochemical data for the MaxEnt simulation.

The Marxan model was implemented at a grid cell resolution of 3000 × 3000 m because the SWAT and MaxEnt outputs were resampled to the same cell size; the gross domestic product (GDP) acquired from the Chinese Academy of Sciences was used as the protection cost of the Marxan model when identifying the priority areas.

Table 1
Summary of data used in this work.

Data	Scale/ Resolution	Data source	Model
DEM	90 m	SRTM Digital Elevation Data[a];	SWAT; MaxEnt
Land use/land cover	1 km	Chinese Academy of Sciences[b];	SWAT
Soil types and soil properties	1 km	Cold and Arid Regions Sciences Data Center at Lanzhou[c];	SWAT; MaxEnt
Daily discharge	3 stations	Hydrological Department (HD)	SWAT
Daily weather	13 stations	China Meteorological Administration	SWAT
Reservoir	7 reservoirs	HD	SWAT
Monthly sediment	1 station	HD	SWAT
Monthly water quality	1 station	HD	SWAT
Crop management practice	–	Statistical Yearbook of Hunan Province	SWAT
Gross domestic product (GDP)	1 km	Chinese Academy of Sciences. Resource and Environment data platform[d];	Marxan
Fish location	–	Hunan Aquatic Ecological Monitoring Programs	MaxEnt
Bioclimatic data	30 s	WorldClim[e]	MaxEnt
Nitrogen and phosphorus pollution inputs	53 sub-basins	Hunan Statistic Yearbook	SWAT
Future climate projections	1 km	WorldClim[e]	SWAT; MaxEnt

[a] Source: http://srtm.csi.cgiar.org/;.
[b] Source: http://www.resdc.cn/;.
[c] Source: http://westdc.westgis.ac.cn;.
[d] Source: http://www.resdc.cn/Default.aspx.
[e] Source: https://www.worldclim.org/.

3.2. WES simulation and visualization

In this study, SWAT was employed to simulate ecohydrological processes representing hydrological and hydrochemical related WES. The MaxEnt model was used to simulate fish distribution representing hydroecological related WES.

The WES related to hydrological processes were selected and calculated based on the SWAT's HRU output file (output.hru) for further analyses (Table S1). The WES we selected for further analysis were based on expert assessments. The experts came from water-related academic fields and were familiar with the environmental characteristics of the XRB. Three types of WES were derived from SWAT, including the water yield (WYLD), the simulated mean sediment yield (SYLD), and the levels of organic nitrogen (ORGN) and organic phosphorus (ORGP) to represent the ecosystem services of 'water flow control', 'erosion control', and 'water purification & nutrient status' in the study area, respectively. These WES represent the essential ecosystem services in the forest-dominated ecosystems in the XRB, providing information for water

Table 2
Mean values (1999–2015) of the WES indicators in different seasons.

Water-related ecosystem service	Indicator	Baseline	Wet season (Mar to Jul)	Dry season (Nov to Feb)
Water flow	WYLD (mm)	65.81	99.94	31.22
Erosion control	SYLD (t/ha)	0.66	1.29	0.30
Water purification & Nutrient status	ORGN (kg N/ha)	0.45	0.89	0.22
	ORGP (kg P/ha)	0.06	0.11	0.03

Note: WYLD: water yield; SYLD: Sediment yield; ORGN: Organic N yield; ORGP: Organic P yield (see text for details).

resource management. The minimum and maximum values of the four indicators for all HRUs were calculated (Table 2).

The SWAT model was calibrated and validated using the historical data collected from three major hydrological stations (Hengyang, Hengshan, and Xiangtan) on the main stream of the Xiangjiang River from January 1997 to December 2015. The periods 1997 to 1998, 1999 to 2005, and 2006 to 2015 were used as warm-up periods, calibration periods, and validation periods, respectively. The coefficient of determination (R^2) and the Nash-Sutcliffe efficiency coefficient (NS) were used to evaluate the accuracy of the SWAT model (R^2 all above 0.51 and NS all above 0.42) (Fig. S1) (Wang et al., 2019).

Because *Ctenopharyngodon idella, Hypophthalmichthys molitrix, Mylopharyngodon piceus*, and *Aristichys nobilis* were the four major Chinese carps in the middle reaches of the Yangtze River and Xiangjiang River is an important habitat of their natural stock resources, we simulated the distribution of those kinds of fishes to represent the hydroecological WES. We initially selected 44 environmental factors (i.e., bioclimatic data, fish occurrence data, topographic data, soil properties, hydrological processes, and water quality) that might affect the extent of suitable fish habitat to model the current fish distributions. Since many variables were spatially correlated, Spearman's rank correlation analysis was conducted to examine the cross-correlation. Variables with highly correlated relationships were removed to avoid multicollinearity. Out of 44 initial variables, 31 were retained as indicator variables (Table 1).

We used the MaxEnt model to simulate the current and future fish distribution in the XRB. We used 75% of the point data for model training and the remaining 25% for validating the model. The area under the receiver operating characteristic curve (AUC) was used to quantify model accuracy. AUC values $\langle$ 0.7 indicate low accuracy, values between 0.7 and 0.9 indicate moderate accuracy, and values $\rangle$ 0.9 denote high accuracy. The AUC value of our MaxEnt model was 0.802.

We mapped the water flow, erosion, water purification status, and fish distribution in the XRB in different climate scenarios using the SWAT and MaxEnt model.

3.3. Systematic conservation planning

The systematic conservation planning model Marxan is a widely used space optimization software for systematic conservation planning. According to the local stakeholder's opinion, we input the regional GDP in 2015 as the financial cost in the Marxan simulation. The goal of the objective function is to minimize the GDP loss to optimize the allocation of the WES-priority areas. A sub-basin with a high GDP is assumed to have (i) limited areas for conserving natural water resources because those areas were overexploited during urbanization; (ii) higher economic losses for allocating crucial conservation zones since many huge infrastructure projects are being constructed here.

Based on the planning units, the total GDP cost was calculated as (more details are provided in the Supplementary Information):

$$Total\ GDP\ cost = \sum_{PUs} GDP\ cost + 60\sum_{PUs} Boundary + \sum_{30\%\ of\ the\ total\ amount\ of\ WES} SPF \times Penalty \quad (1)$$

where *PU* represents the planning units, and *SPF* refers to the conservation feature penalty factor.

The Marxan model was used to identify the WES-priority areas and obtain the conservation values of the planning units in the XRB under various climate change scenarios. The results of the Marxan model under different climate scenarios were obtained, and the WES-priority areas and the selection time of the priority areas (Fig. S3) were optimized. The results were summarized by determining the best solution (the conservation network with the optimum locations meeting the objectives at minimum cost) for all climate scenarios. We also evaluated the frequency of selecting the planning units from 100 runs in each climate scenario to evaluate the irreplaceability, which is defined as the likelihood of the given location having a specific set of protection objectives.

We adopted the method of Xu et al. (2013) to evaluate the conservation efficiency of the WES-priority areas under different climate change scenarios:

$$SE = \left(\frac{E_p}{E}\right) \Big/ \left(\frac{S_p}{S}\right) \quad (2)$$

where *SE* denotes the spatial conservation efficiency of the WES; E_p describes the total WES of the identified priority areas, *E* represents the total WES in the region, S_p is the area of WES-priority areas, and *S* is the total area. An *SE* index greater than 1 indicates high conservation efficiency and vice versa.

3.4. Key factors determining the spatial pattern of WES-priority areas

Based on the level of sub-basins, the redundancy analysis (RDA) was conducted to investigate the impact of climate change (precipitation and temperature), topography (altitude and slope), GDP, and land use (forestland, grassland, cropland, built-up land, and water) on the WES-priority area's selection. The analysis was implemented using the RDA modules embedded in the CANOCO software (version 4.5&5.0, Ithaca, USA).

The integrity index (PI) and aggregation index (AI) calculated by the FRAGSTATS software were used to determine the dispersion of the WES-priority areas (He et al., 2000).

4. Results and discussion

4.1. Spatial distribution of hydrological and hydrochemical related WES in three climate change scenarios

The WYLD, SYLD, ORGN, and ORGP all reached the highest values in the wet season (from March to July) and the lowest in the dry season (from November to February) (Table 2). As the result of intensified precipitation, the WYLD was 99.94 mm in the wet season, which was three times the amount in the dry season. The values of the SYLD, ORGN, and ORGP were four times higher in the wet season than in the dry season. The highest average value of SYLD in the wet season was 1.29 t/ha. Since surface runoff is higher in the wet season due to high-intensity precipitation, soil erosion was higher (Casazza et al., 2018). In the XRB, farming practices are mainly carried out during wet seasons. The large amount of effluents from agricultural activities in the wet season carries nutrient-rich moisture, such as nitrogen and phosphorus, to the XRB. Thus, the values of ORGN and ORGN were higher in wet seasons (Zhang et al., 2019). Moreover, frequent rainfall in wet season could further increase decomposition and nutrient release from the natural plants and soil profiles, which is another reason causing the higher outputs of ORGN and ORGP (Yan et al., 2019). The seasonal variation of WES did not have a substantial impact on the spatial distribution of ecosystem services in the XRB but had a significant impact on ecosystem service values (Fig. 3). Generally, as the rainfall increased between March and July and the flood season of the Xiangjiang River approached, the values of the four ecosystem service indicators increased.

Most areas that were not forestland had relatively low water flow values due to high runoff coefficients in those regions (Fig. 3a) (Liu et al., 2020). Since forestland has a higher soil water retention capacity than other types of LULC, more runoff occurs than in non-forest land during floods (Malekian and Azarnivand, 2016). Higher values of SYLD were found in high-elevation grassland in the southwest and north of the XRB, whereas the lowest SYLD values were observed in areas with flat terrain and low rainfall (Fig. 3b). Since grasslands do not have a tree canopy to intercept raindrops or litter layers to prevent splashing during rain events, the higher sediment yield was not surprising (Zhou et al., 2016). Moreover, highly erosive areas were mostly found in cropland,

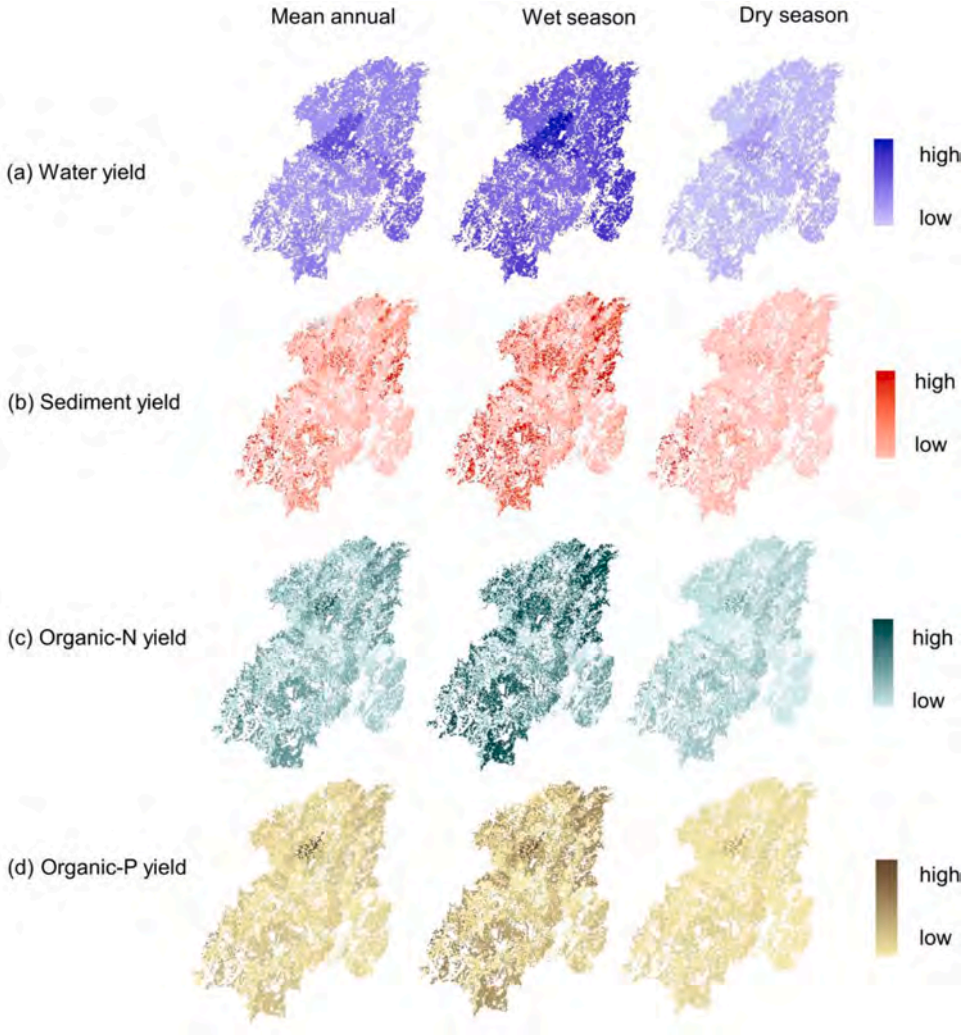

Fig. 3. Maps of the WES surrogates in the SWAT model in the baseline scenario (1999–2015). (a) Water yield representing the water flow; (b) sediment yield representing erosion control; (c) organic-N yield, and (d) organic-P yield representing water purification & nutrient status.

especially in valleys with steep slopes and high annual rainfall. Opening up wastelands could be one reason for the high erosion (Xie et al., 2019). Besides, high-intensity rainfall loosens soil particles, which are transported with the water downhill into streams and valleys (Pimentel and Burgess, 2013). The most common soil type in this area is Alisol, which is unstable and prone to erosion. The lower erosion levels of cultivated fields demonstrated the protective role of row crops for soil and water conservation. The ORGN and ORGP reached their maximum values (0.903 kg/ha and 0.111 kg/ha, respectively) in the southern areas, where their spatial patterns were similar to SYLD (Fig. 3c). Specifically, the largest values occurred in agricultural and forest areas, indicating that they were the primary sources of ORGN and ORGP. The spatial patterns of the four WES in the mid-term and long-term scenarios are shown in Fig. S2. In the future climate scenarios, the lower values of the WYLD were found in the southcentral areas, and the areas with low values decreased from 2050 to 2070. Compared to 2050, the southern regions with steeper slopes showed the higher level of WYLD in 2070. The SYLD, ORGN, and ORGP had similar spatial patterns between 2050 and 2070. The highest values of those indices occurred in the south (0.378 t/ha, 0.639 kg/ha, and 0.078 kg/ha, respectively for mid-term; 0.364 t/ha, 0.662 kg/ha, and 0.081 kg/ha, respectively for long-term).

4.2. Spatial distribution of hydroecological related WES in three climate change scenarios

In the current climate scenario, the most suitable areas for fish species were found in the freshwater reaches of the main stem of the Xiangjiang River in the downstream section (Fig. 4). The remaining regions in the XRB had lower suitability or were deemed unsuitable for fish. The outputs indicated that the fish were distributed in the lower to medium elevations in the current climatic condition. The model predicted that the most suitable areas for fish in 2050 would be located in the middle mainstream of the Xiangjiang River and the downstream tributaries in the eastern section of the basin. In 2070, the optimum locations for fish survival would be located in the upper mainstream and parts of the branches in the middle valley, increasing the range following climate warming. These results were consistent with recent studies that predicted species would move to higher elevations to adjust to the future climate (McMahan et al., 2020). Barriers such as waterfalls could prevent species from moving upstream, restricting species movements and threatening their lives. Higher values of ORGN, ORGP, and SYLD were found in the southern areas, indicating lower suitability for fish. Higher levels of ORGN and ORGP may cause eutrophication, which may result in the total depletion of oxygen and the generation of harmful gasses, such as hydrogen sulfide and methane, threatening fish survival (Nyenje et al., 2010). The accumulation of sediments may adversely impact spawning, inhibit migration, and interfere with food intake (Kukuła and

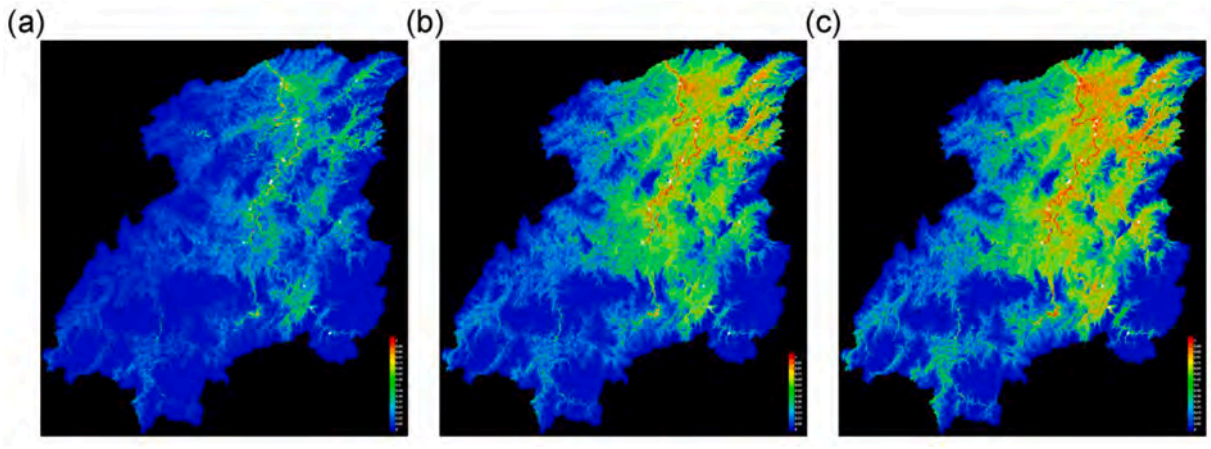

Fig. 4. Fish distribution in the baseline scenario (a), mid-term scenario (b), and (c) long-term scenario.

Bylak, 2020).

4.3. Systematic conservation planning utilizing WES-priority areas

4.3.1. Identifying priority areas for multiple WES

The output of the Marxan model indicated that the spatial distribution of the WES-priority areas differed for different climate scenarios (Fig. 5), and the overlap between the area in different scenarios was about 13% of the total area. Most of the overlap occurred in the south and east of the study area. Since forest land accounted for 60% of the study area, it substantially affected water cycle and nutrient cycle in the entire study area. Thus, priority areas were centered in forest land with higher altitudes in the eastern XRB. Priority areas were also found at the source of the rivers in the southern portion of the XRB; thus, these areas require sufficient attention and protection. Priority areas located in the central area of the XRB during the baseline scenario shifted to the downstream area in the mid-term and long-term scenarios due to high water flow in the middle and upper reaches of the XRB as a result of climate change. The number of patches and the average patch size of the WES-priority areas in three climate change scenarios were 15 and 1214 km^2 (baseline), 19 and 1053 km^2 (mid-term), and 22 and 837 km^2 (long-term), respectively.

In each climate change scenario, the patches of the WES-priority areas were clustered, and their overall PI and AI were 99.01 and 96.52 (baseline), 99.177 and 96.5911 (mid-term), and 98.94 and 96.15 (long-term), respectively, indicating the largest clustering effect in the mid-term scenario. Moreover, the WES-priority areas were more dispersed in the long-term climate scenarios than in the baseline scenario.

The conservation efficiency index of the WES-priority areas is listed in Table 3. The index was the highest for the baseline climate scenario. The WES-priority areas with the highest values were located in the upper reaches of the XRB (south and southeast of the study area). The average conservation efficiency of the WES-priority areas was lower in the climate change scenarios than the baseline scenario. In the mid-term and long-term climate scenarios, the conservation efficiency was less than 1, indicating an adverse effect of climate change.

4.4. The social-environmental factors associated with the location of the WES-priority areas

4.4.1. The effect of climatic factors on WES-priority area selection

The results of the analysis of the impact factors and characteristics of climate change on the WES-priority areas are shown in Fig. 6a. Precipitation and temperature were selected as key variables to represent the impact of climate change (Fig. 6a-1, b-1, and c-1). A positive correlation between precipitation and WYLD is observed in the scatterplot. Studies have shown that an increase in precipitation in the future significantly improved the WYLD, affecting certain priority areas (Shirmohammadi et al., 2020). The cumulative proportion of precipitation was 18.4% in

Table 3
Conservation efficiency of WES in three climate change scenarios.

Scenarios	Average conservation efficiency
Baseline (1999–2015)	1.264
Mid-term (2050)	0.937
Long-term (2070)	0.867

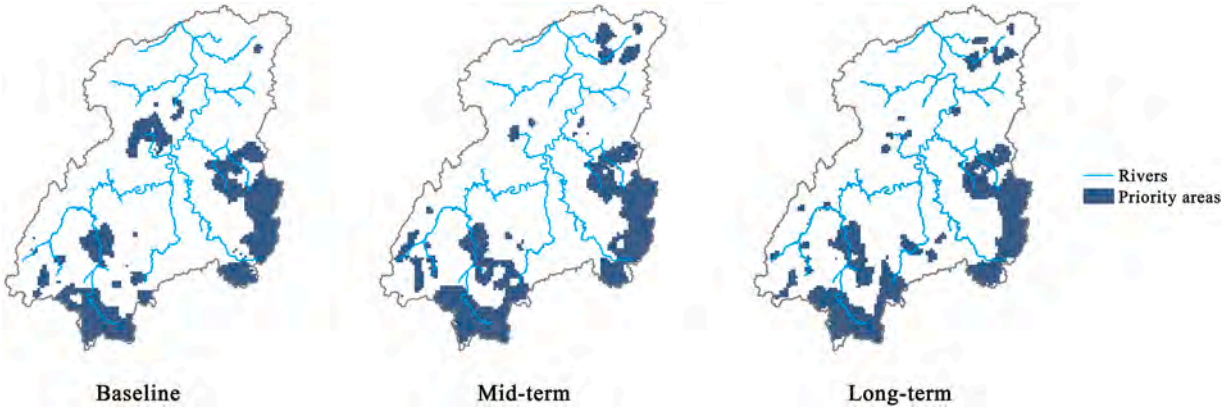

Fig. 5. Priority areas for conserving multiple WES in all climate scenarios.

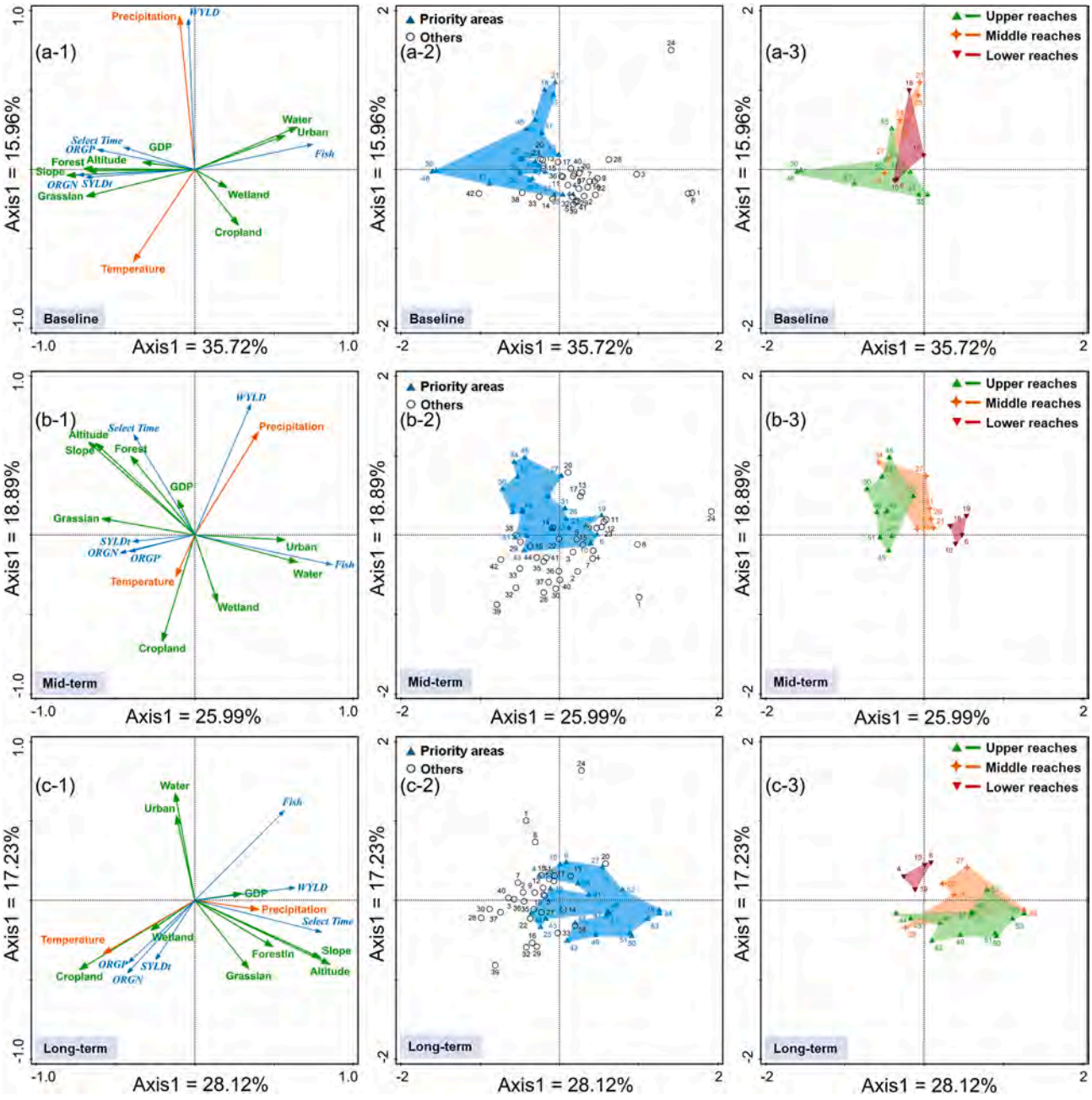

Fig. 6. RDA ordination diagram based on the spatial-temporal variability of the priority areas under three climate change scenarios. (a) baseline; (b) mid-term; (c) long-term. Different groupings are enclosed in polygons based on the priority areas (a-2, b-2, c-2) and the priority areas in different locations in the Xiangjiang River Basin (a-3, b-3, c-3).

XRB. Moreover, the fish distribution was positively correlated with the precipitation in all climatic scenarios. Our result is consistent with previous study that fish distribution correlated positively with precipitation (Kinard et al., 2021). These findings suggest that aridification is linked to the extinction of competitive and environmentally sensitive taxa, potentially resulting in less favorable community states.

In the baseline climate scenario, the average air temperature was below 20 °C (Table S2). The angle between the selected WES-priority areas and the temperature in the graph was almost vertical, indicating that the temperature had a negligible effect on the WES-priority areas (Fig. 6a-1). In contrast, in the mid-term scenario, the WES-priority areas were highly and negatively correlated with the temperature (Fig. 6b-1), and the correlation was even higher in the long-term climate scenario (Fig. 6c-1). In the Mediterranean island of Crete, 3 °C warming caused a reduction in water resources by 10–30% (Koutroulis et al., 2016). In addition, a variable infiltration capacity (VIC) model was used to simulate WYLD in different temperature scenarios. The results showed that the streamflow sharply decreased as the temperatures increased (Weltzin et al., 2003). Our results show a negative relationship between temperature and WYLD under future climate scenarios confirmed those results. The positive correlation between temperature and nutrient outputs (ORGN & ORGP) was found in all climatic scenarios. It might be attributed to the fact that the farming practices are mainly carried out when temperature is higher. The effluents from cultivation carry nutrient-rich moisture to the XRB. Numerous studies have also suggested that the increased temperature may hasten the mineralization of soil organic matter, which releases dissolved nutrients, particularly nitrogen and phosphorus (Andriamananjara et al., 2019).

4.4.2. The social and economic factors affecting the distribution of the WES-priority areas in different reaches

Since downstream water users rely on the upstream water supply, it is crucial to understand the differences in the WES-priority area distributions in different reaches. The number of WES-priority areas and their distribution differ in the upper, middle, and lower reaches of the XRB (Fig. S4).

Climate change had a negligible impact on the WES-priority area's distribution in the upstream basin of the XRB. In the upper basins of the XRB with rugged terrain, the topographic factors were crucial factors influencing the selection of the upstream WES-priority areas, particularly the slope, whose cumulative slope proportion was 20.9% (Fig. 6a). The selection of WES-priority areas with steep slopes and high altitudes in the upper basin of the XRB was slightly affected by climate change (Fig. 6a-3, b-3, and c-3). The regions with steep slopes and high altitudes are mainly the source of the rivers in the upper basin; thus, these areas require sufficient attention and protection in all the climate scenarios, which is in agreement with a previous study (Crossman et al., 2012). Besides, the upper basin of the XRB contained most of the WES-priority areas (Fig. 6a-3, b-3, and c-3). Thus, decision-makers and stakeholders should focus on WES-priority areas in the upper reaches.

The WES-priority areas proportion in the middle reaches declined from 6.4% in the baseline scenario to 5.6% in the mid-term and 4.5% in the long-term, respectively (Fig. 5 and Fig. 6a-3, b-3, and c-3). The middle reaches, including rapidly developing counties that have large areas of cropland and many urban areas, are areas where urbanization may increase due to a population boom and industrialization. Therefore, large amounts of readily available water will be required. The WES-priority areas selection is closely related to the WYLD in that areas in all scenarios (Figs. 1 and 6). As climate change accelerates, the available water supply in some parts of the middle reach will decrease (Table 3); thus, these areas may not require future protection and will not be selected as WES-priority areas. Moreover, the agricultural planting in the middle reaches could promote global warming, because a considerable increase in crop yield resulting from increased irrigation and fertilizer application may cause increased greenhouse gas emissions (Liu et al., 2005). Since the selection of the WES-priority areas are strongly and negatively correlated with the temperature (Fig. 6), the WES-priority areas proportion in that areas decreases over time. Overall, because of the incremental demand for water resources in the middle reaches, there is a need to consider the influence of future climate on hydrological factors for modifying water resources management schemes (Mirdashtvan et al., 2021).

Relatively few WES-priority areas are located in the lower reaches in all climate scenarios. The downstream basin is the social and economic center of Hunan province, whose economy is well developed compared to other basins, with a high urbanization level (Ying et al., 2007). The WES-priority areas distribution of the lower reaches is relevant with the built-up land and GDP (Fig. 6), all of which could explain 14.7% of the total variance maximumly, confirming the above results. The high urbanization in the lower reaches results in a high proportion of impervious areas. Further, the aquifers in this area were destroyed by excessive exploitation during economic development. Therefore, there are few places suitable for WES-priority areas. The number of WES-priority areas is inadequate in the lower reaches in all scenarios. A large proportion of the water resources for many citizens comes from the tributary of the Xiangjiang River, i.e., the Liuyang River (Yang et al., 2020). Priority areas 6 and priority areas 10 are located in the watershed of the Liuyang River. Those regions should be considered as WES-priority areas in all scenarios to meet the water demand of the population in the central city. Both the water quality and WYLD are important aspects that should be evaluated in those regions.

The clustering degree of the WES-priority areas is also dependent on climate change. The WES-priority areas have relatively high similarity and high aggregation in the mid-term climate scenario. In contrast, in the long-term scenario, the WES-priority areas are less similar and less clustered (Fig. 6b-2 and c-2). This result is consistent with the WES-priority area's location (Fig. 5). The low aggregation and dispersed distribution of the WES-priority areas could increase their protection costs, causing difficulties for management and maintenance (Hawkins, 2004).

5. Conclusions

In this study, a novelty framework was proposed to integrate WES into the water resource priority areas management under climate change. Furthermore, the hydrological/hydrochemical/hydroecological processes in the integrated terrestrial–aquatic system were also considered. In the climate change scenarios, the priority management areas were concentrated in the southern and southeastern regions of the upper reaches. The conservation efficiency of the WES-priority areas declined over time. The precipitation was positively correlated with the WES-priority area selection in all climate scenarios. The temperature was only negatively correlated with the WES-priority areas when it exceeded 20 °C, and this effect became more pronounced as the temperature increased.

In the upper basin, the topographic factors were the most crucial factors for the selection of the upstream WES-priority areas. Thus, the WES-priority area selection was only slightly affected by climate change. In the middle basin, the WES-priority area's selection was closely related to the WYLD in all scenarios, and the number of priority areas in that area declined along with climate change. Relatively few WES-priority areas were located in the lower reaches in all climate scenarios, and WES-priority areas were positively associated with the GDP and the amount of built-up land. According to this study, to preserve healthy aquatic and terrestrial ecosystems, the elements of hydrology, hydrochemistry, and hydroecology should be addressed in the selection of priority areas.

Declaration of Competing Interest

The authors declare no conflict of interest.

Data availability

Data will be made available on request.

Acknowledgments

This work was supported by the National Natural Science Foundation of China (51979101, 72088101, 51679082, 51521006, 51809184), the Hunan Science & Technology Innovation Program (2018RS3037), the Natural Science Foundation of Hunan Province (2019JJ20002) and the Three Gorges Follow-up Research Project (2017HXXY-05).

Supplementary materials

Supplementary material associated with this article can be found, in the online version, at doi:10.1016/j.watres.2022.118766.

References

Andriamananjara, A., Chevallier, T., Masse, D., Razakamanarivo, H., Razafimbelo, T., 2019. Land management modifies the temperature sensitivity of soil organic carbon, nitrogen and phosphorus dynamics in a Ferralsol. Appl. Soil Ecol. 138, 112–122. https://doi.org/10.1016/j.apsoil.2019.02.023.

Baker, T.J., Miller, S.N., 2013. Using the Soil and Water Assessment Tool (SWAT) to assess land use impact on water resources in an East African watershed. J. Hydrol. 486, 100–111. https://doi.org/10.1016/j.jhydrol.2013.01.041 (Amst).

Balkanlou, K.R., Müller, B., Cord, A.F., Panahi, F., Malekian, A., Jafari, M., Egli, L., 2020. Spatiotemporal dynamics of ecosystem services provision in a degraded ecosystem: a systematic assessment in the Lake Urmia basin, Iran. Sci. Total Environ. 716, 137100 https://doi.org/10.1016/j.scitotenv.2020.137100.

Casazza, M., Lega, M., Liu, G., Ulgiati, S., Endreny, T.A., 2018. Aerosol pollution, including eroded soils, intensifies cloud growth, precipitation, and soil erosion: a review. J. Clean. Prod. 189, 135–144. https://doi.org/10.1016/j.jclepro.2018.04.004.

Crossman, N.D., Bryan, B.A., Summers, D.M., 2012. Identifying priority areas for reducing species vulnerability to climate change. Divers. Distrib. 18, 60–72. https://doi.org/10.1111/j.1472-4642.2011.00851.x.

de Loë, R.C., Murray, D., Brisbois, M.C., 2016. Perspectives of natural resource sector firms on collaborative approaches to governance for water. J. Clean. Prod. 135, 1117–1128. https://doi.org/10.1016/j.jclepro.2016.06.166.

Frederico, R.G., De Marco, P., Zuanon, J., 2014. Evaluating the use of macroscale variables as proxies for local aquatic variables and to model stream fish distributions. Freshw. Biol. 59, 2303–2314. https://doi.org/10.1111/fwb.12432.

Hawkins, D.E., 2004. A protected areas ecotourism competitive cluster approach to catalyse biodiversity conservation and economic growth in Bulgaria. J. Sustain. Tour. 12, 219–244. https://doi.org/10.1080/09669580408667235.

He, H.S., DeZonia, B.E., Mladenoff, D.J., 2000. An aggregation index (AI) to quantify spatial patterns of landscapes. Landsc. Ecol. 15, 591–601. https://doi.org/10.1023/A:1008102521322.

He, P., Li, J., Li, Y., Xu, N., Gao, Y., Guo, L., Huo, T., Peng, C., Meng, F., 2021. Habitat protection and planning for three Ephedra using the MaxEnt and Marxan models. Ecol. Indic. 133, 108399.

Hockley, F.A., Wilson, C.A.M.E., Brew, A., Cable, J., 2014. Fish responses to flow velocity and turbulence in relation to size, sex and parasite load. J. R. Soc. Interface 11, 20130814. https://doi.org/10.1098/rsif.2013.0814.

Huang, F., Wang, X., Lou, L., Zhou, Z., Wu, J., 2010. Spatial variation and source apportionment of water pollution in Qiantang River (China) using statistical techniques. Water Res. 44, 1562–1572. https://doi.org/10.1016/j.watres.2009.11.003.

Jiang, Y., 2009. China's water scarcity. J. Environ. Manag. 90, 3185–3196. https://doi.org/10.1016/j.jenvman.2009.04.016.

Kim, Z., Shim, T., Koo, Y.M., Seo, D., Kim, Y.O., Hwang, S.J., Jung, J., 2020. Predicting the impact of climate change on freshwater fish distribution by incorporating water flow rate and quality variables. Sustainability 12, 10001. https://doi.org/10.3390/su122310001.

Kinard, S., Patrick, C.J., Carvallo, F., 2021. Effects of a natural precipitation gradient on fish and macroinvertebrate assemblages in coastal streams. PeerJ 9, e12137. https://doi.org/10.7717/peerj.12137.

Koutroulis, A.G., Grillakis, M.G., Daliakopoulos, I.N., Tsanis, I.K., Jacob, D., 2016. Cross sectoral impacts on water availability at +2°C and +3°C for east Mediterranean island states: the case of Crete. J. Hydrol. 532, 16–28. https://doi.org/10.1016/j.jhydrol.2015.11.015 (Amst).

Kukuła, K., Bylak, A., 2020. Synergistic impacts of sediment generation and hydrotechnical structures related to forestry on stream fish communities. Sci. Total Environ. 737, 139751 https://doi.org/10.1016/j.scitotenv.2020.139751.

Liang, J., He, X., Zeng, G., Zhong, M., Gao, X., Li, Xin, Li, Xiaodong, Wu, H., Feng, C., Xing, W., Fang, Y., Mo, D., 2018. Integrating priority areas and ecological corridors into national network for conservation planning in China. Sci. Total Environ. 626, 22–29. https://doi.org/10.1016/j.scitotenv.2018.01.086.

Liang, J., Li, S., Li, X., Li, X., Liu, Q., Meng, Q., Lin, A., Li, J., 2021. Trade-off analyses and optimization of water-related ecosystem services (WRESs) based on land use change in a typical agricultural watershed, southern China. J. Clean. Prod. 279 https://doi.org/10.1016/j.jclepro.2020.123851.

Liang, J., Liu, Q., Zhang, H., Li, Xiaodong, Qian, Z., Lei, M., Li, Xin, Peng, Y., Li, S., Zeng, G., 2020. Interactive effects of climate variability and human activities on blue and green water scarcity in rapidly developing watershed. J. Clean. Prod. 265, 121834 https://doi.org/10.1016/j.jclepro.2020.121834.

Liu, J., Liu, M., Tian, H., Zhuang, D., Zhang, Z., Zhang, W., Tang, X., Deng, X., 2005. Spatial and temporal patterns of China's cropland during 1990–2000: an analysis based on Landsat TM data. Remote Sens. Environ. 98, 442–456. https://doi.org/10.1016/j.rse.2005.08.012.

Liu, W., Li, Z., Zhu, J., Xu, C., Xu, X., 2020. Dominant factors controlling runoff coefficients in karst watersheds. J. Hydrol. 590, 125486 https://doi.org/10.1016/j.jhydrol.2020.125486 (Amst).

Luo, Z., Shao, Q., Zuo, Q., Cui, Y., 2020. Impact of land use and urbanization on river water quality and ecology in a dam dominated basin. J. Hydrol. 584, 124655 https://doi.org/10.1016/j.jhydrol.2020.124655 (Amst).

Maes, W.H., Heuvelmans, G., Muys, B., 2009. Assessment of land use impact on water-related ecosystem services capturing the integrated terrestrial–aquatic system. Environ. Sci. Technol. 43, 7324–7330. https://doi.org/10.1021/es900613w.

Malekian, A., Azarnivand, A., 2016. Application of integrated shannon's entropy and VIKOR techniques in prioritization of flood risk in the Shemshak Watershed, Iran. Water Resour. Manag. 30, 409–425. https://doi.org/10.1007/s11269-015-1169-6.

Malekian, A., Choubin, B., Liu, J., Sajedi-Hosseini, F., 2019. Development of a new integrated framework for improved rainfall-runoff modeling under climate variability and human activities. Water Resour. Manag. 33, 2501–2515. https://doi.org/10.1007/s11269-019-02281-0.

McMahan, C.D., Fuentes-Montejo, C.E., Ginger, L., Carrasco, J.C., Chakrabarty, P., Matamoros, W.A., 2020. Climate change models predict decreases in the range of a microendemic freshwater fish in Honduras. Sci. Rep. 10, 12693. https://doi.org/10.1038/s41598-020-69579-7.

Mekonnen, M.M., Hoekstra, A.Y., 2016. Four billion people facing severe water scarcity. Sci. Adv. 2, e1500323 https://doi.org/10.1126/sciadv.1500323.

Mirdashtvan, M., Najafinejad, A., Malekian, A., Sa'doddin, A., 2021. Sustainable water supply and demand management in semi-arid regions: optimizing water resources allocation based on RCPs Scenarios. Water Resour. Manag. 35, 5307–5324. https://doi.org/10.1007/s11269-021-03004-0.

Mirdashtvan, M., Najafinejad, A., Malekian, A., Sa'doddin, A., 2018. Downscaling the contribution to uncertainty in climate-change assessments: representative concentration pathway (RCP) scenarios for the South Alborz Range, Iran. Meteorol. Appl. 25, 414–422. https://doi.org/10.1002/met.1709.

Nyenje, P.M., Foppen, J.W., Uhlenbrook, S., Kulabako, R., Muwanga, A., 2010. Eutrophication and nutrient release in urban areas of sub-Saharan Africa — A review. Sci. Total Environ. 408, 447–455. https://doi.org/10.1016/j.scitotenv.2009.10.020.

Pimentel, D., Burgess, M., 2013. Soil erosion threatens food production. Agriculture 3, 443–463. https://doi.org/10.3390/agriculture3030443.

Richter, B.D., Mathews, R., Harrison, D.L., Wigington, R., 2003. Ecologically sustainable water management: managing river flows for ecological integrity. Ecol. Appl. 13, 206–224, 10.1890/1051-0761(2003)013[0206:ESWMMR]2.0.CO;2.

Rosenfeld, J.S., 2017. Developing flow–ecology relationships: implications of nonlinear biological responses for water management. Freshw. Biol. 62, 1305–1324. https://doi.org/10.1111/fwb.12948.

Schmalz, B., Kruse, M., Kiesel, J., Müller, F., Fohrer, N., 2016. Water-related ecosystem services in Western Siberian lowland basins—analysing and mapping spatial and seasonal effects on regulating services based on ecohydrological modelling results. Ecol. Indic. 71, 55–65. https://doi.org/10.1016/j.ecolind.2016.06.050.

Shirmohammadi, B., Malekian, A., Salajegheh, A., Taheri, B., Azarnivand, H., Malek, Z., Verburg, P.H., 2020. Impacts of future climate and land use change on water yield in a semiarid basin in Iran. Land Degrad. Dev. 31, 1252–1264. https://doi.org/10.1002/ldr.3554.

Sutherland, A.B., Meyer, J.L., 2007. Effects of increased suspended sediment on growth rate and gill condition of two southern Appalachian minnows. Environ. Biol. Fishes 80, 389–403.

Tian, Y., Xu, Y.P., Wang, G., 2018. Agricultural drought prediction using climate indices based on support vector regression in Xiangjiang River basin. Sci. Total Environ. 622–623, 710–720. https://doi.org/10.1016/j.scitotenv.2017.12.025.

Wang, Q., Liu, R., Men, C., Guo, L., Miao, Y., 2019. Temporal-spatial analysis of water environmental capacity based on the couple of SWAT model and differential evolution algorithm. J. Hydrol. 569, 155–166. https://doi.org/10.1016/j.jhydrol.2018.12.003 (Amst).

Wei, J., Wei, Y., Western, A., 2017. Evolution of the societal value of water resources for economic development versus environmental sustainability in Australia from 1843 to 2011. Glob. Environ. Change 42, 82–92. https://doi.org/10.1016/j.gloenvcha.2016.12.005.

Weltzin, J.F., Loik, M.E., Schwinning, S., Williams, D.G., Fay, P.A., Haddad, B.M., Harte, J., Huxman, T.E., Knapp, A.K., Lin, G., Pockman, W.T., Shaw, R.M., Small, E.E., Smith, M.D., Smith, S.D., Tissue, D.T., Zak, J.C., 2003. Assessing the response of terrestrial ecosystems to potential changes in precipitation. Bioscience 53, 941–952, 10.1641/0006-3568(2003)053[0941:ATROTE]2.0.CO;2.

Xie, Y., Lin, H., Ye, Y., Ren, X., 2019. Changes in soil erosion in cropland in northeastern China over the past 300 years. Catena 176, 410–418. https://doi.org/10.1016/j.catena.2019.01.026.

Xu, H., Xu, C.Y., Chen, H., Zhang, Z., Li, L., 2013. Assessing the influence of rain gauge density and distribution on hydrological model performance in a humid region of China. J. Hydrol. 505, 1–12. https://doi.org/10.1016/j.jhydrol.2013.09.004 (Amst).

Xu, W., Xiao, Yi, Zhang, J., Yang, W., Zhang, L., Hull, V., Wang, Z., Zheng, H., Liu, J., Polasky, S., Jiang, L., Xiao, Yang, Shi, X., Rao, E., Lu, F., Wang, X., Daily, G.C., Ouyang, Z., 2017. Strengthening protected areas for biodiversity and ecosystem services in China. Proc. Natl. Acad. Sci. USA 114, 1601. https://doi.org/10.1073/pnas.1620503114.

Yan, F., Sun, Yongjian, Hui, X., Jiang, M., Xiang, K., Wu, Y., Zhang, Q., Tang, Y., Yang, Z., Sun, Yuanyuan, Jun, M., 2019. The effect of straw mulch on nitrogen, phosphorus and potassium uptake and use in hybrid rice. Paddy Water Environ. 17, 23–33. https://doi.org/10.1007/s10333-018-0680-9.

Yang, J., Zhang, C., Fu, J., Wang, S., Ou, X., Xie, Y., 2020. Pre-grouting reinforcement of underwater karst area for shield tunneling passing through Xiangjiang River in Changsha, China. Tunn. Undergr. Space Technol. 100, 103380 https://doi.org/10.1016/j.tust.2020.103380.

Ying, X., Zeng, G.M., Chen, G.Q., Tang, L., Wang, K.L., Huang, D.Y., 2007. Combining AHP with GIS in synthetic evaluation of eco-environment quality—A case study of Hunan Province, China. Ecol. Model. 209, 97–109. https://doi.org/10.1016/j.ecolmodel.2007.06.007.

Zhang, X., Lin, C., Zhou, X., Lei, K., Guo, B., Cao, Y., Lu, S., Liu, X., He, M., 2019. Concentrations, fluxes, and potential sources of nitrogen and phosphorus species in atmospheric wet deposition of the Lake Qinghai Watershed, China. Sci. Total Environ. 682, 523–531. https://doi.org/10.1016/j.scitotenv.2019.05.224.

Zhou, J., Fu, B., Gao, G., Lü, Y., Liu, Y., Lü, N., Wang, S., 2016. Effects of precipitation and restoration vegetation on soil erosion in a semi-arid environment in the Loess Plateau, China. CATENA 137, 1–11. https://doi.org/10.1016/j.catena.2015.08.015.